Design of Band-Notched MIMO Antenna for UWB Applications

Ahmed Shaker[1] and Ayman Haggag[2]
[1] Faculty of Engineering, Helwan University, Cairo, Egypt
[2] Faculty of Industrial Education, Helwan University, Cairo, Egypt
Email: ahmed_shaker@h-eng.helwan.edu.eg, haggag@techedu.helwan.edu.eg

Abstract—A compact ultra-wideband (UWB) Multiple-Input-Multiple-Output (MIMO) antenna with a notched band is presented. The proposed design consists of four unipolar UWB radiators, and these monopole radiators are placed perpendicular to each other to exploit polarization diversity, where the four-element ultra-wideband (UWB) Multiple-Input-Multiple-Output (MIMO) antenna is presented. The total size of the antenna is 60x60 mm^2. The operating frequency of the antenna is 3.1–11 GHz with a return loss of less than 10 dB, except at the notched band of 4.9– 5.9 GHz. This antenna consists of an isosceles trapezoidal plate with a circular notch cut and two transitional steps as well as a partial ground plane. For UWB bandwidth enhancement techniques: use of a partial ground plane, and modify the gap between the radioactive element and ground plane technique, using steps to control the resistance stability and a notch cut technique. The notch cut from the radiator is too used to reduce the size of the plane antenna. The measured -10 dB return loss bandwidth for the designed antenna is about 116.3% (8.7 GHz). The MIMO antenna does not require any additional structure to improve insulation. The proposed antenna supplies an acceptable radiation pattern and relatively flat gain over the entire frequency band.

***Index Terms*—**Multiple Input Multiple Output (MIMO), Ultra-wide Band (UWB), Notched UWB, CST

I. Introduction

There are a lot of common services nowadays the customers would like to have in their terminals such as Internet access, video streaming, games downloading files, etc. However, all these services require a higher data rate transmission than conventional voice calls. The world's leading companies in mobile communications have given a huge force to the development of 4G wireless systems to satisfy the customers' demand for high data rates, quality of transmission, and accuracy. MIMO antenna system is a key feature enabling technology for fourth-generation (4G) wireless communication [1]. This technology has become a good solution to fulfill the demand for high data rate and to improve the performance of future wireless communication systems [2], and This is primarily because MIMO systems can increase channel capacity with an increase in the number of the elements [3], without additional bandwidth or transmit power.

MIMO is a key component of standards of wireless communication, such as IEEE 802.11 (Wi-Fi), Long Term Evolution (LTE), and Worldwide Interoperability for Microwave Access (WiMAX) [4], [5]. MIMO has raised interest because of its applications in 4G, RFID, Digital Home, and WLAN. Demand for high data rate, as a result, is to increase the huge bandwidth. To improve the system's capability, a very broadband MIMO antenna was developed for commercial systems.

MIMO antenna systems are heavily implemented in wireless devices to enhance channel capacity and multipath propagation [6]. The UWB MIMO antenna has high application isolation in automotive communication systems and radar imaging systems [7], [8]. Recently, a Multi-Input-Multi-Output (MIMO) order has been proposed, to increases channel capacity, allowing multiple users to access various services at the same time [9]-[10].

The idea of MIMO is that the sample signals in the spatial domain are combined at both transmitter and receiver receptors to form multiple streams of parallel spatial data that increase the rate of data. The occurrence of diversity also improves the quality that is the bit-error-rate (BER) of the communication [11]. Using UWB technology, wireless devices can transmit a very wide range of bandwidth while consuming less power [12]. Also, the UWB technology-based devices have many other advantages, including high data rates, increased bandwidth, and low cost [13]. It is designed UWB antennas for portable devices. Planar antennas are a promising solution for UWB applications because of their simple design, low cost, and performance [13]. Many UWB- MIMO antennas are presented in [14], [15], Most of these MIMO antennas were without notched or need techniques to reduce the coupling between the elements.

This paper presents a compact MIMO antenna with a bandwidth from 3.1 to 11.6 GHz for UWB applications with a notched band at WLAN services. It has a compact size of 60 $\times$ 60 mm^2. Two planar-monopole antennae are placed with guides to direct a perpendicular optical wave perpendicular to each other compared to the conventional UWB antenna; the proposed antenna collects the advantages of the orthorhombic structure and the separation structure to achieve a low joint coupling and a compact size.

Manuscript received August 1, 2020; revised December 16, 2020.
doi:10.12720/jcm.16.1.1-7

II. Antenna Design

A. UWB Antenna

The design of a single UWB radiator is presented in [16]. Fig. 1 shows the geometry of a single radiator which is fed by 50 Ω microstrip line. The substrate is selected to be Rogers RT/ Duroid 5880 material with a relative permittivity ε_r =2.2 and a thickness of 1.575 mm. The radiator shape is chosen to be trapezoidal; it can show a UWB characteristic. Where the initial parameters are calculated using the following empirical formula reported in [16] after adding the effect of the substrate:

$$f_L(GHz) = \frac{904}{(4\pi h + w + w_1)} \quad (1)$$

where

f_L: the frequency corresponding to the lower edge of the bandwidth for the trapezoidal sheet.

W and W_1: the width of the trapezoidal patch bases.

h: the height of the trapezoidal patch

TABLE I: THE OPTIMIZED DIMENSIONS OF THE UWB ANTENNA

No	Parameter	Value
1	Thickness of substrate	1.575mm
2	Length of the substrate, Lsub	30mm
3	Width of the substrate, Wsub	30mm
4	Width trapezoidal patch1, w	28mm
5	Width trapezoidal patch2, w_1	20mm
6	Width trapezoidal patch3, w_2	14mm
7	Length trapezoidal patch1, h	10.5mm
8	Length trapezoidal patch2, h_1	2mm
9	Length trapezoidal patch3, h_2	3mm
10	Length feed, L_f	12mm
11	Width feed, W_f	3.6mm
12	Ground Plane length, L_g	11mm
13	Ground Plane width, W_g	30mm
14	Radius The notched, r	7mm

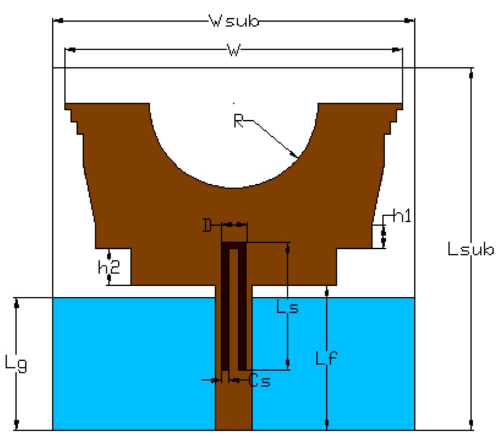

Fig. 1. The initial geometry of UWB antenna

Table I presents the optimized dimensions of the UWB antenna. The dimensions are expressed in mm. This formula is used to foresee the lower edge frequency of the bandwidth for the trapezoidal sheet hanging in the space on the ground plane. It is accurate to +/- 9 % for frequencies in the range of 500 MHz to 6 MHz. The sheet will be a patch printed on a substrate, so, the effect of the substrate has to be incorporated into the formula. After adding it, the formula becomes:

$$f_L(GHz) = \frac{904}{(4\pi h + w + w_1)\sqrt{\varepsilon_{\mathrm{reff}}}} \quad (2)$$

where the effective relative permittivity ε_{eff} can be calculated using:

$$\varepsilon_{eff} = (\varepsilon_r + 1)/2 \quad (3)$$

where

ε_r: The relative permittivity of the substrate

Since the antenna is designed for UWB, it has to operate over 3.1 - 10.6 GHz

B. Notched UWB Antenna Design

After design the UWB antenna, the U-shape slot is etched on the radiator element to achieve a notched band at WLAN operating frequency. Fig. 2 shows the parameters of the U-shape slot; the dimensions of the U-slot are optimized to give the required notched band from frequency 5GHz to 6GHz which are used for WLAN service. The optimized dimensions of the global best and the fabricated value of the U-shaped slot are listed in Table II.

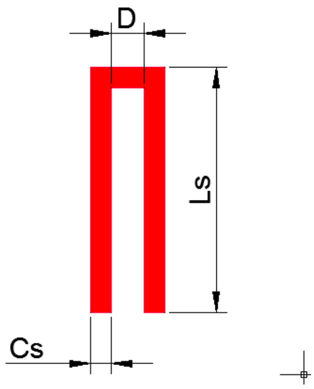

Fig. 2. U-shaped slot for the notched band

$$\text{Fitness (J)} = \min\left(\sum_{f=3GHz}^{5GHz}|S_{11}(f)| - \sum_{f=5GHZ}^{6GHz}|S_{11}(f)| + \sum_{f=6GHZ}^{11GHz}|S_{11}(f)|\right) \quad (4)$$

The fitness function as in (4) minimizes the reflection coefficient $|S_{11}|$ overall UWB spectrums (below -10 dB) and maximize $|S_{11}|$ over the notched band (over -10dB).

TABLE II: OPTIMIZED DIMENSIONS OF U-SLOT

NO	Parameter	Value
1	Length of notched, L_s	10.4mm
2	Width of notched, d	0.7mm
3	Thickness of notched, C_S	0.45mm
4	Distance from the beginning, s	5mm

The band notched feature can be postulated as in

$$f_{notch} = \frac{c}{2L\sqrt{\varepsilon_{eff}}} \quad (5)$$

where c is the speed of light, $L = D + 2 * L_s - 2 * C_s$ is the total length of the U-slot and ε_{eff} is the effective dielectric constant given by (6)

$$\varepsilon_{eff} = \frac{\varepsilon_r + 1}{2} \qquad (6)$$

Fig. 3 shows the picture of the fabricated UWB antenna with notched band characteristic on Rogers RT/Duroid 5880 material substrate with a size of 30mm by 30mm.

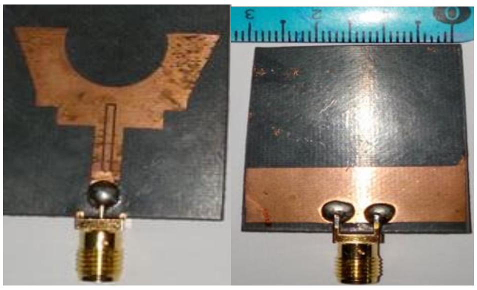

Fig. 3. The picture of the notched UWB antenna

C. UWB MIMO Antenna

Fig. 4 shows the antenna layout, which is made of four UWB antennas, which are placed clockwise and be vertical to each other to form the body of the MIMO antenna with size 60 x 60 mm^2. The proposed antenna consists of four single-slot U-shaped radiators. The first antenna was placed in a U-shaped slot radiator perpendicular to the second antenna. Similarly, the second U-shaped slot radiator was placed perpendicular to the other radiator at the self-same space and the second U-shaped slot radiator was placed vertically to the third, U-shaped slot radiator was placed perpendicular to the other radiator at the same distance. These slots were used to improve the broadband matching. The antennas were placed this way to achieve broadband matching characteristics, polarization diversity, and high isolation. Later on, the ground planes of all these radiators were connected through a shortening is fed by a microstrip line 12 mm long and 3.6 mm wide. The impedance matching in the 3.1–11 GHz frequency range was achieved. The antenna has a compact size and the orthogonality of the element achieves the reduction of mutual coupling between the elements.

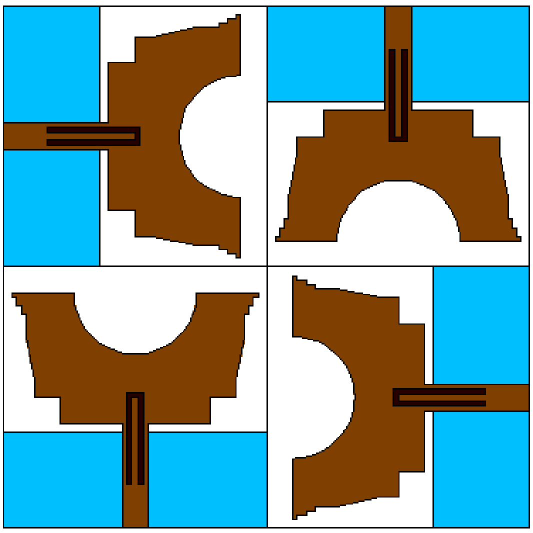

Fig. 4. The Geometry of optimum MIMO UWB antenna

III. Results and Discussions

A. UWB Antenna

Fig. 5 shows the measured reflection coefficient $|S_{11}|$ compared with the simulated results for a UWB antenna utilize CST simulation. Performance is gained since the measured values of the return loss is very close to the simulated one in most of the extent of the frequency band. It is noted that the antenna can support different resonance patterns, and it is closely distributed across the spectrum, so the interference of these resonance media leads to the UWB property.

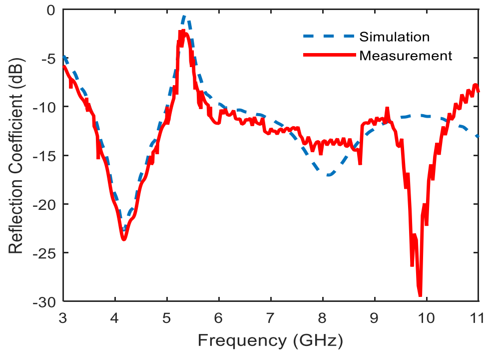

Fig. 5. The simulated and measured reflection coefficients of the UWB antenna

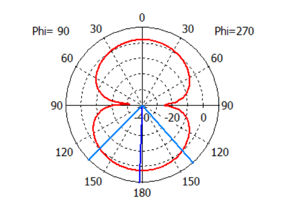	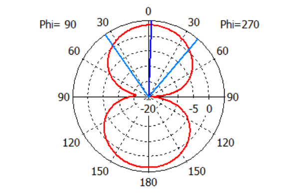
Far-field (f=3 GHz) Main lobe magnitude =2.24 dBi Main lobe direction= 178.0 deg. Angular width (3 dB)= 86.5 deg.	Far-field (f=5.2GHz) Main lobe magnitude= 3.51 dBi Main lobe direction2.0 deg. Angular width (3 dB)= 75.6 deg.
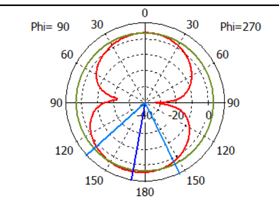	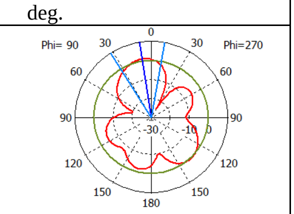
Far-field (f=7GHz) Main lobe magnitude= 4.34 dBi Main lobe direction= 170.0 deg. Angular width (3 dB)= 73.5 deg. Side lobe level = -0.8dB	Far-field (f=11GHz) Main lobe magnitude= 1 dBi Main lobe direction= 9.0 deg. Angular width (3 dB)= 42.2 deg. Side lobe level = -1.0 dB

Fig. 6. The simulation radiation pattern of notched UWB antenna in xz- and yz- plans

Typical the antenna radiation patterns at 3 GHz and 7 GHz and 11 in xy -plane are plotted in Fig. 6. The antenna has a dipole-like radiation pattern that confirms that it is operating in the primary resonance mode. Fig. 7 shows the simulated of the VSWR which indicates the notch at the required frequency band.

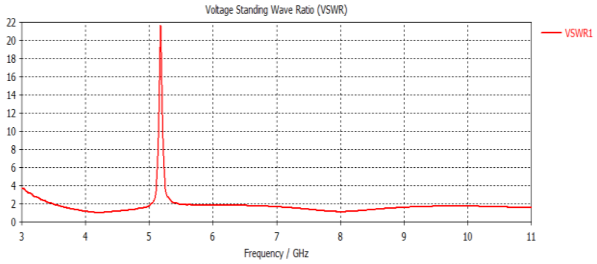

Fig. 7. The simulated VSWR of the UWB antenna

B. *UWB MIMO Antenna*

Fig. 8 shows the reflection coefficients simulated results of the MIMO antenna. When the first element is excited, the surface current occurs strongly on the corresponding element resulting in a rise of the mutual coupling. The mutual coupling can be reduced by increasing the distance between elements. However, this will result in the big size of the suggested MIMO antenna.

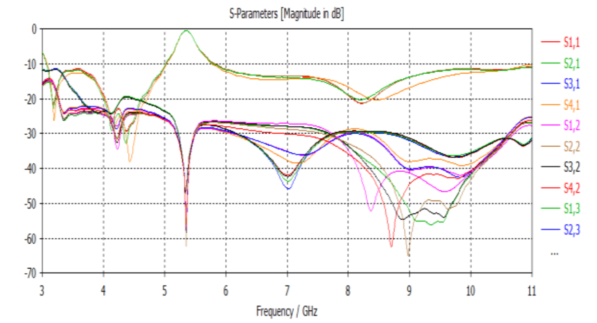

Fig. 8. The simulated S-parameters of the MIMO antenna elements

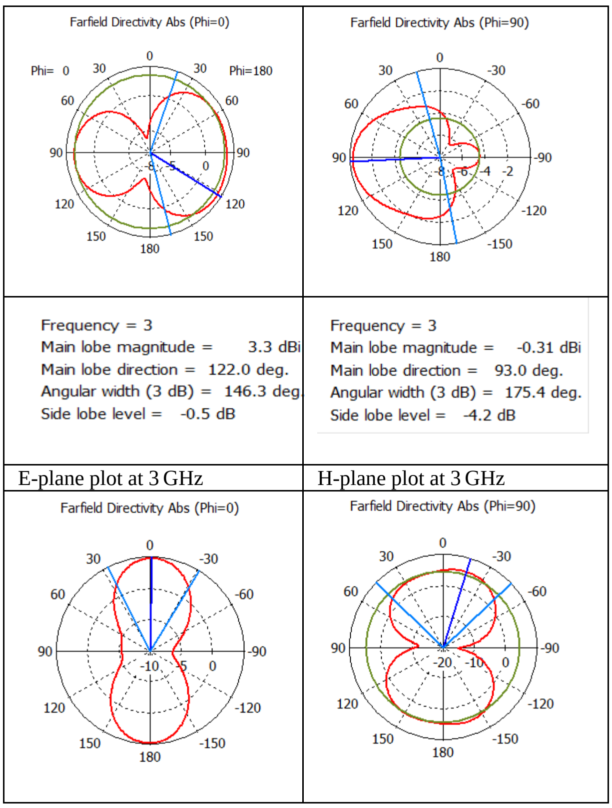

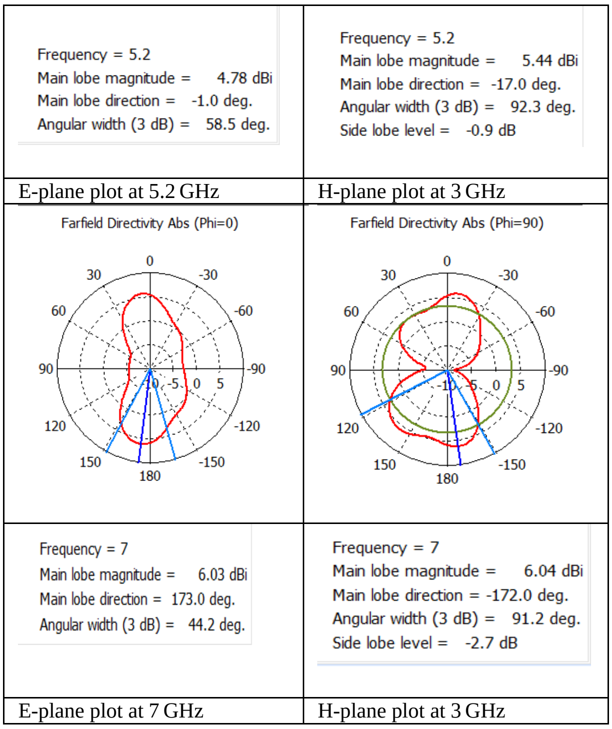

Fig. 9. The simulation radiation pattern of the MIMO antenna in xz- and yz- planes at frequencies

Fig. 9. describes E-plane (phi=0) and H-plane (phi=90) plots of the MIMO antenna system at the frequencies 3GHz and 5.2Hz and 7Hz.

Fig. 10. shows the 3-D Radiation pattern of the MIMO antenna system describing all the four ports at 7 GHz

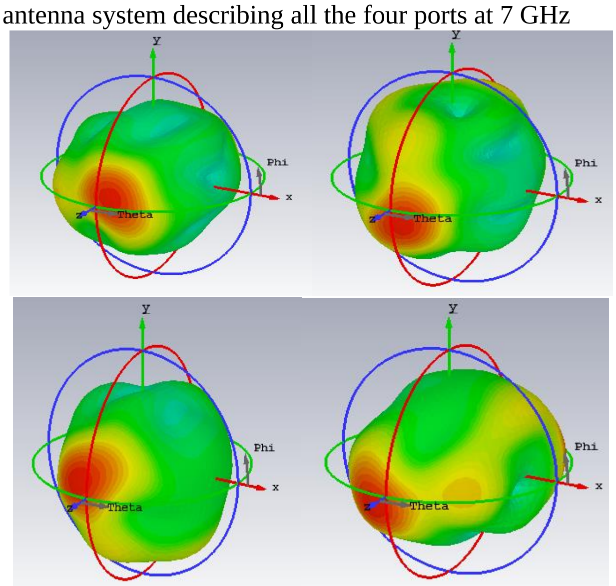

Fig. 3-D radiation pattern of the MIMO antenna at 7 GHz of all the ports

Fig. 11 depicts the simulated gain of the antenna. The gain varies from 1.6 dB to 5.8 dB over the operating frequency range. It can be concluded that the gain variation is 4.2dB over the entire operating frequency range, the radiation efficiency of the antenna is specified by the radiated power, and the input force accepted by the antenna. It was thence observed that the maximum radiation qualification was 5.85 dB at 7 GHz.

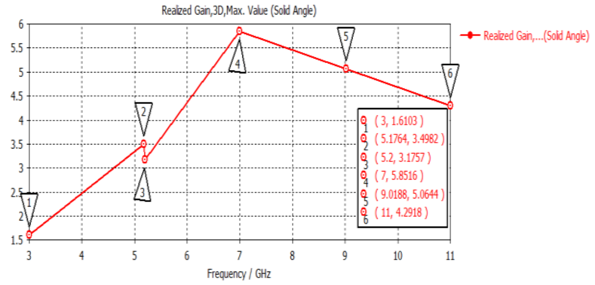

Fig. 11. The antenna gain versus frequency

Fig. 12 shows the picture of the fabricated UWB MIMO antenna. The measured reflection coefficients of the MIMO antenna are shown in Fig. 13. From this format, it was noted that the antenna could operate over the extended range from 3 GHz to 11 GHz and shows at WLAN frequency band from 4.9 GHz to 5.9 GHz, the antenna gives good rejection.

Fig. 12. The picture of the fabricated UWB MIMO antenna

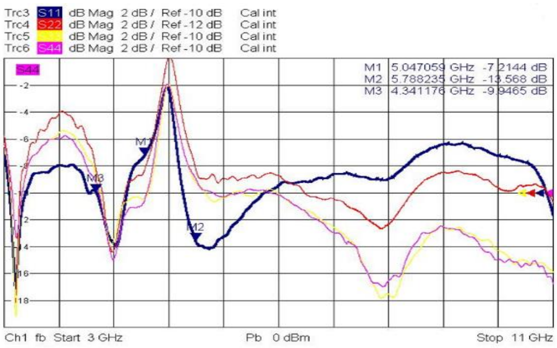

Fig. 13. The measured reflection coefficients of the MIMI antenna

Fig. 14 shows the simulated and measured S-parameters of the antenna for biased states. Where Fig. 14 (a) shows the simulated and measured S_{11} and S_{33}, and Fig. 14 (b) shows the simulated and measured S_{22} and S_{44}. The results indicate an acceptable match between each measured and simulation results, and that the antenna gives a matched impedance for UWB frequencies with the notched band at the frequencies used in WLAN services.

Fig. 15 shows the measured results of the mutual coupling of the final MIMO antenna. The measured results show that the mutual coupling between cross- (1,2) and polarization elements (1,3) is less than −17 dB and −16 dB over the UWB range, respectively. It is observed that the measured results are in good agreement with the simulated results. the results show that the mutual coupling of the cross- and polarization elements of the final MIMO antenna are less than −10 dB. Any discrepancy is attributed to manufacturing tolerance. These results prove that this antenna is a good candidate for MIMO operation across the UWB band.

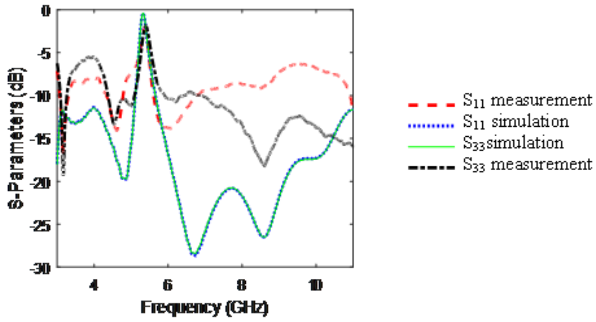

(a)

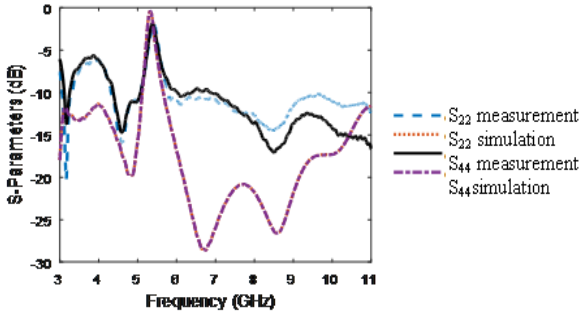

(b)

Fig. 14. The measured and the simulated S- parameters, (a) S_{11} and S_{33}, (b) S_{22} and S_{44}

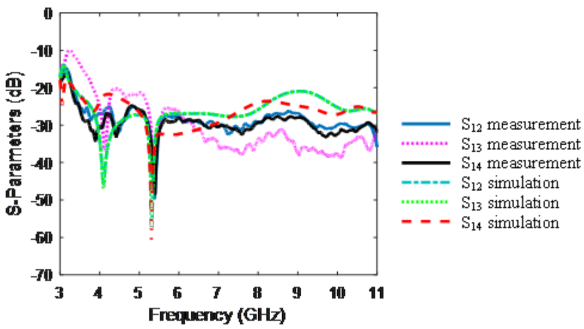

(a)

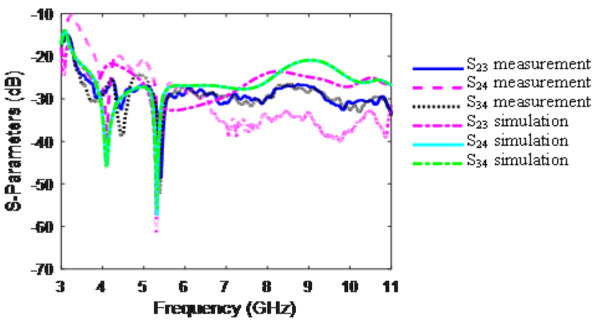

(b)

Fig. 15. The measured and simulated mutual coupling. (a) S_{12}, S_{13}, and S_{14}, (b) S_{23}, S_{24}, and S_{34}

IV. CONCLUSION

Compact UWB-MIMO antenna arrays with four radiating elements have been proposed in this article. The MIMO antenna design has a band-stop design on the bottom side and four radiators share a ground plane using a rectangular shortening strip .The technology is used to design a UWB-MIMO antenna with an irregular shape radiator with a notched band characteristic. The antenna built on a Rogers RT/Duroid 5880 substrate with 60 × 60 mm^2 surface area, 1.575 mm thickness with a relative permittivity, ε_r=2.2, and loss tangent of 0.02 and can cover the UWB spectrum (3.1-11 GHz) with a notched band from 4.9 GHz to 5.9 GHz with stable radiation characteristics. In the future work, the antenna can be more compact and can utilize the use of electromagnetic bandgap (EBG) to reduce the mutual coupling in the array elements.

Conflict of Interest

The authors declare no conflict of interest.

Author Contributions

All authors conducted the research; analyzed the data; wrote the paper; and all authors have approved the final version.

References

[1] M. S. Sharawi, "Printed multi-band MIMO antenna systems and their performance metrics," *IEEE Magazine of Antennas and Propagation*, vol. 55, no. 5, pp. 218-232, 2013.

[2] G. Foschini and M. Gans, "On limits of wireless communications in a fading environment when using multiple antennas," *Wireless Personal Communications*, vol. 6, pp. 311-335, 1998.

[3] D. Gesbert, M. Shafi, D. Shiu, P. J. Smith, and A. Naguib, "From theory to practice: An overview of MIMO space-time coded wireless systems," *IEEE Journal on Selected Areas in Communications*, vol. 21, no. 3, pp. 281-302, 2003.

[4] 3GPP Technical Specification (TS) Group, "Spatial channel model, SCM-134 text V6.0," *Spatial Channel Model AHG*, Apr. 2003.

[5] V. Erceg, *et al*., "IEEE 802.16 broadband wireless access working group," IEEE 802.16.3c-01/29r4, 2001.

[6] A. Kumar and A. Chaudhary, "Channel capacity enhancement of wireless communication using MIMO technology," *International Journal of Scientific & Technology Research*, vol. 1, no. 2, 2012.

[7] L. Hui, J. Xiong, and Z. Ying, "Compact and low profile co-located MIMO antenna structure with polarization diversity and high port isolation," *Electronics Letters*, vol. 46, no. 2, pp. 108-110, 2010.

[8] L. Liu, S. Cheung, and T. Yuk, "Compact MIMO antenna for portable devices in UWB applications," *IEEE Trans. on Antennas and Propagations*, vol. 61, no. 8, pp. 4257–4264, 2013.

[9] A. Goldsmith, S. A. Jafar, N. Jindal, and S. Vishwanath, "Capacity limits of MIMO channels," *IEEE Journal on Selected Areas in Communications*, vol. 21, no. 5, pp. 684-702, 2003.

[10] L. Zheng and D. Tse, " Diversity and multiplexing: A fundamental tradeoff in multiple-antenna channels," *IEEE Trans. on Information Theory*, vol. 49, no. 5, pp. 1073–1096, 2003.

[11] E. Bjornson and B. Ottersten, "A framework for training-based estimation in arbitrary correlated rician MIMO channels with Rician disturbance," *IEEE Trans. on Signal Processing*, vol. 58, no. 3, pp. 1807-1820, 2010.

[12] W. FCC, "DC, Revision of Part 15 of the Commission's rules regarding ultra-wideband transmission systems," *Third Report Order FCC*, FCC 10-151, 2010.

[13] A. M. Abbosh, H. K. Kan, and M. E. Bialkowski "Compact ultra-wideband planar tapered slot antenna for use in a microwave imaging system," *Microwave and Optical Technology Letters*, vol. 48, no. 11, pp. 2212-2216, 2006.

[14] L. Y. Nie, X. Q. Lin, Z. Q. M. Yang, J. Zhang, and B. Wang, "Structure-Shared planar UWB MIMO antenna with high isolation for mobile platform," *IEEE Trans. on Antennas and Propagation*, vol. 67, no. 4, pp. 2735–2738, 2019.

[15] A. T. José, J. Hildeberto, R. Arturo, A. Luis, and G. Ricardo, "Four ports wideband drop-shaped slot antenna for MIMO applications," *Journal of Electromagnetic Waves and Applications*, vol. 34, no. 9, pp. 1159-1179, 2020.

[16] M. A. Hafez, A. Haggag, A. Shaker, and S. Singy, "Optimized interference cancelation based stepped-trapezoidal notched UWB antenna," *Automatic Control and System Engineering Journal*, vol. 18, no. 2, pp. 39-44, 2018.

Ahmed Shaker was born in Cairo, Egypt, on February 10, 1976. He received the B.Sc. and M.Sc. degrees from Helwan University in 1999 and 2006 respectively. His Ph.D. degree from Helwan University, Egypt in 2013. He is currently an assistant professor in the Department of Electronics and Communications Engineering in the Faculty of Engineering, Helwan University, Egypt. His research interests at present include Antennas design, UWB antennas, MIMO antenna, Passive MIMO antenna, mobile communications, and Optimization techniques.

Ayman Haggag was born in Cairo, Egypt in 1971. He received his B.Sc. degree from Ain Shams University, Egypt, in June 1994, M.Sc. degree from Eindhoven University of Technology, The Netherlands, in December 1997, and Ph.D. degree from Chiba University, Japan, in September 2008. Presently, he is an Associate Professor of Communications Engineering at the Electronics Technology Department, Faculty of Technology and Education, Helwan University, Egypt. His current research interests are in the fields of Network Security, Wireless Security, Software Defined Networking and Wireless Sensor Networks.